Reaction Sintering of Ca_2SiO_4–$CaZrO_3$ Composites

D. L. Callahan,* Gareth Thomas

Materials and Chemical Sciences Division, Lawrence Berkeley Laboratory, and Department of Materials Science and Mineral Engineering, University of California at Berkeley, Berkeley, California 94720, USA

J. S. Moya & Pilar Pena

Instituto de Ceramica y Vidrio (CSIC), 28500 Arganda del Rey, Madrid, Spain

Abstract

The reaction sintering mechanism for dicalcium silicate–calcium zirconate composites (C_2S–CZ) has been examined following three different processing routes in order to elucidate the reaction processes and optimize the flexural strength of the ceramic. Fired compacts have been characterized by three-point bend tests, X-ray diffraction, and various techniques of electron microscopy. The phase evolution has been examined by X-ray diffraction of samples fired at temperatures in the range of 1000–$1600°C$.

The highest bend strength attained was $264\,MPa$ in $15\,vol.\%$ C_2S containing composites prepared by a two-stage firing process. Alumina additions facilitate the complete reaction in a single firing process and result in strengths only slightly less than those obtained using the two-stage process. A basic single-stage firing process resulted in incomplete reaction and a very low strength ($\sim 70\,MPa$). The dominant microstructural features which influence sintering and strength in all three cases appear to be phases arising out of the reaction between calcia and silica (and alumina where present).

Der Reaktionssintermechanismus zur Herstellung von Dicalciumsilikat–Calciumzirkonat-Verbundwerkstoffen (C_2S–CZ) wurde mittels dreier verschiedener Verfahren mit dem Ziel untersucht, die Reaktionsprozesse zu beleuchten und die Biegebruchfestigkeiten der Keramik zu optimieren. Die gesinterten Preß körper wurden durch Dreipunkt-Biegebruchversuche, Röntgendiffraktometrie und verschiedene elektronen- mikroskopische Techniken charakterisiert. Die röntgen- diffraktometrische Untersuchung der Phasenentwick-

lung wurde an Proben mit Sintertemperaturen zwischen 1000–$1600°C$ vorgenommen.

Die höchste Biegebruchfestigkeit von $264\,MPa$ wurde an Verbundwerkstoffen mit $15\,Vol.\%$ C_2S, die in einem zweistufigen Sinterprozeß hergestellt wur- den, erreicht. Die Zugabe von Aluminiumoxid- additiven erleichtert das vollständige Reagieren in einem einzigen Sinterprozeß und ergibt Festigkeiten, die nur geringfügig unter denjenigen des zweistufigen Prozesses liegen. Ein normaler, einstufiger Sinter- prozeß ergab eine unvollständige Reaktion und eine sehr geringe Festigkeit ($\sim 70\,MPa$). Die wichtigsten mikrostrukturellen Merkmale, die in allen drei Fällen die Sintereigenschaften und die Festigkeiten beeinflus- sen, scheinen Phasen darzustellen, die aus der Reaktion von Calciumoxid mit Siliziumoxid (sowie Aluminiumoxid, wo vorhanden) entstehen.

On a étudié le mécanisme de frittage de composites silicate de dicalcium–zirconate de calcium (C_2S–CZ) en empruntant trois voies d'élaboration différentes, afin d'identifier les mécanismes réactionnels et d'optimiser la résistance à la flexion de la céramique. Les échantillons frittés ont été caractérisés par des essais de flexion trois points, par diffraction RX et par différentes techniques de microscopie électronique. L'évolution des phases a été suivie par diffraction RX d'échantillons portés à des températures comprises entre 1000 et 1600°C.

On a obtenu une résistance en flexion maximum de $264\,MPa$ dans des composites contenant 15% en volume de C_2S et élaborés par un frittage comportant deux étapes. Des ajouts d'alumine facilitent une réaction totale dans le cas d'un frittage en une étape et conduisent à des résistances seulement légèrement plus faibles que dans le cas d'un frittage en deux étapes. Un frittage élémentaire en une étape conduit à une réaction incomplète et à une résistance faible

* Present address: Department of Mechanical Engineering and Materials Science, Rice University, Houston, Texas 77251, USA.

397

*(≃ 70 MPa). Les éléments microstructuraux domi-
nants, influençant dans les trois cas le frittage et la
résistance mécanique, semblent être les phases produ-
ites par la réaction entre la silice et la calcite (et
l'alumine quand elle est présente).*

1 Introduction

Dicalcium silicate (Ca_2SiO_4, abbreviated C_2S)–
calcium zirconate ($CaZrO_3$, abbreviated CZ) com-
posites may be produced in a range of C_2S:CZ
compositions having enhanced strength compared
to bulk CZ and enhanced mechanical stability
compared to bulk C_2S.[1] One of the attractive
features of these ceramics is the potential for direct
reaction sintering to form the composites from
initial mixtures of calcia, silica and zirconia as
deduced from the CaO–SiO_2–ZrO_2 ternary phase
diagram.[2,3] Other interesting features of these
composites include relatively high coefficients of
thermal expansion (for $C_2S > 1.5 \times 10^{-5}$)[4] and
possible toughening induced by the β- to γ-C_2S
transformation. This study details three methods of
processing these ceramics and examines the relation-
ships between the processing and resultant micro-
structures and strengths.

The direct reaction sintering process between
calcia and zircon takes place in the solid state as
deduced from the relevant equilibrium phase

Processing Routes

Fig. 1. C_2S–CZ reaction sintering process routes.

diagrams and the relatively low temperatures of
reaction. The final microstructures may conse-
quently be very much dependent upon the com-
position and microstructure of the starting powders.

A basic reaction process will be examined which
relies entirely upon the direct solid-state reaction
between initial powders to form the final ceramic.
A two-stage firing process involving rehomo-
genization after prereaction will also be studied. The
additional steps are designed to mitigate the effects
of any local concentrations of silica or calcia isolated
after formation of the majority CZ phase. The
temperatures for prereaction will be determined by
studying the phase evolution in the basic process
held at different firing temperatures. Finally, the
effect of alumina as a sintering additive in the direct
reaction sequence will be investigated.

2 Experimental Procedures

Three processing routes are shown schematically in
Fig. 1. The starting powders were identical in all
three cases, being calcium carbonate ($CaCO_3$,
Probus, Spain) and zirconia-enriched zircon (ZrO_2 .
$0.14 SiO_2$, Zedox 10, Anzon Ltd, UK) mixed
following the formula

$$ZrO_2 . 0.14 SiO_2 + 1.28 CaCO_3 \rightarrow$$
$$CaZrO_3 + 0.14 Ca_2SiO_4 + 1.28 CO_2(g)$$
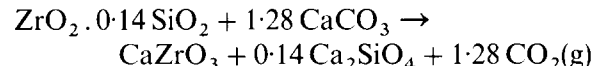
Taking into account the solid-state compatibility
relations in the system ZrO_2–SiO_2–CaO.[1-3] (Fig. 2),
the studied composition lies on the CZ–C_2S solid-
state compatibility join.

In this study crystalline calcia is obtained by the
in-situ decomposition of calcium carbonate. Silica
and zirconia are introduced in a silica-leached,
plasma-decomposed zircon (Zedox 10). The zircon
in such powders is for the most part decomposed
into large aggregates of fine monoclinic zirconia
particles and amorphous silica.[5,6] Consequently,
after homogenization by attrition milling the solid-
state reactions forming CZ and C_2S may be
considered to occur relatively independently, the
former taking place between calcia and monoclinic
zirconia and the latter between calcia and amorph-
ous silica. Additional reactions are predicted only
between calcia and the silica, where a broad range of
calcium silicates might arise due to local inhomo-
geneities.

In the basic process the starting powders were
mixed and then attrition milled with zirconia (Mg-
PSZ) balls in alcohol (2-propanol) for 1 h, followed
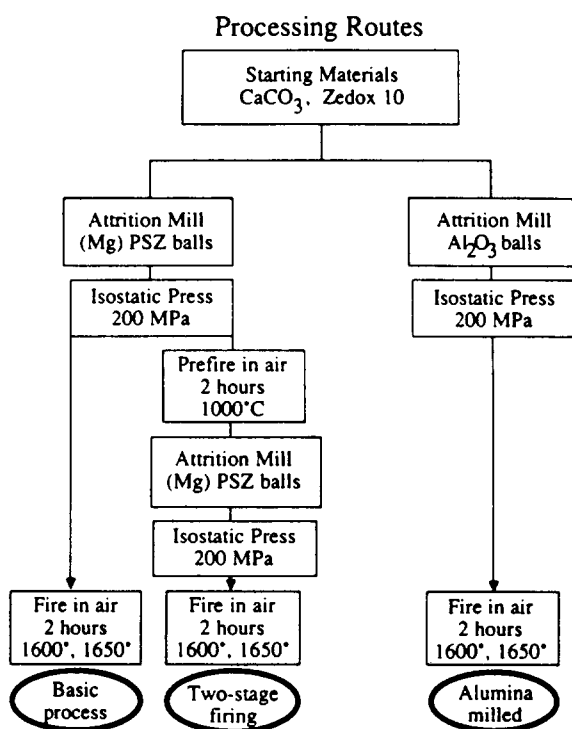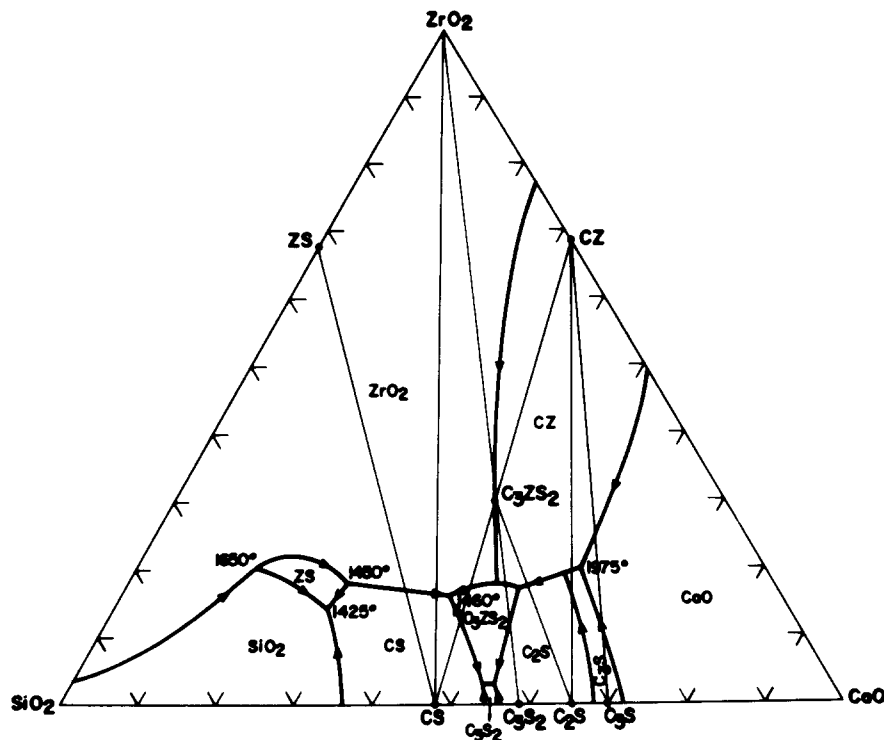by drying and sifting. The powders were then

Fig. 2. Phase equilibrium of the system CaO–SiO$_2$–ZrO$_2$.

isostatically pressed at 200 MPa into cylindrical bars and fired for 2 h at 1650°C. In each case the samples were held for 2 h at 850°C for CaCO$_3$ decomposition. The two-stage process essentially followed through these same steps twice in series with the first firing at 1000°C and the final firing (after rehomogenizing and pressing) at 1650°C. The alumina-milled process differed from the basic process only in that alumina balls were used to dope the starting powders with alumina during attrition milling. After firing, wet chemical analyses were performed on samples obtained by each different processing route.

At temperatures above approximately 1525°C this small amount of alumina added to calcia should form a calcia-rich melt stable in contact with crystalline calcia. Similar stable liquid phases are expected for small amounts of alumina added to silica or dicalcium silicate at temperatures above approximately 1600 and 1550°C respectively.[3] Such liquid phases should be stable at the chosen reaction temperature and thus significantly enhance mass transport and facilitate the formation of equilibrium phases through liquid state diffusion of the soluble species.

The bulk density of fired samples was determined by the water displacement method and the phase composition by X-ray diffraction (XRD). XRD was also used to characterize the phase evolution of the composites by examining ceramics produced using the basic reaction process with lower firing temperatures (in the 1000 to 1200°C range). The bend strengths (σ_f) were determined by three-point bend tests on cylindrical specimens of approximately 3 mm diameter.

The microstructures of the composites were examined by backscatter electron imaging in the scanning electron microscope (SEM; model JCM-35CF, Jeol USA, Inc., Peabody, MA), by conventional transmission electron microscopy (TEM; model EM400T, Philips Instruments, Eindhoven, The Netherlands) in conjunction with energy dispersive X-ray spectroscopy (EDS; model 8000 Analyst, Kevex, Foster City, CA). Specimens were produced as thin foils following standard procedures for thinning ceramics (cutting, polishing, dimpling, ion milling) and were carbon coated to avoid charging under the electron beam.

3 Results

The bend strengths and bulk density measurements are tabulated in Table 1 for composites from each processing type and the corresponding wet chemical analyses are presented in Table 2. The three types of

Table 1. Properties of 15 vol.% C$_2$S composites

	σ_f (MPa)	ρ (g/cm^3)
Basic process	70 ± 10	3·77
Two-stage firing	264 ± 10	4·03
Alumina milled	241 ± 18	4·1

Table 2. Wet chemical analysis of trace elements (wt%)

	Basic process[a]	Alumina-milled
Al_2O_3	0·14	0·30
Fe_2O_3	0·15	0·18
TiO_2	0·14	0·13
Na_2O	0·06	0·04
MgO	0·02	0·05
K_2O	0·05	0·01

[a] Zirconia-milled.

composites will be discussed independently here and more general comparisons and conclusions examined in later sections.

3.1 Basic process

Composites produced by this basic reaction sintering process were very soft to the touch and prone to cracking with a very low bend strength (~ 70 MPa after 2 months) as noted in Table 1. X-Ray diffraction patterns following the evolution of these phases at firing temperatures from 1000 to 1200°C are shown in Fig. 3. A small peak indicating unreacted zirconia is present in patterns from composites fired at 1000 and 1100°C and com-

parison of this peak to the prominent CZ peak shows that the CZ producing reaction will take place and be essentially completed at temperatures in this range. XRD results indicated the expected presence of CZ but a poor signal-to-noise ratio made conclusive statements about the minority C_2S phase impossible. The presence of $CaCO_3$ is probably due to carbonation of the free lime remaining in the sample at 1000°C (Fig. 3). TEM examination of these composites clearly showed the presence of the CZ phase, some very small amounts of C_2S and considerable amounts of amorphous calcium silicate phases and unreacted calcia. These amorphous regions were typically found separating the CZ and C_2S phases from unreacted calcia grains, as shown in Fig. 4.

3.2 Two-stage firing

This process was adopted to enhance the C_2S-forming reactions by rehomogenizing the mixtures after the partial formation of CZ and the formation of amorphous reaction barriers about the unreacted calcia grains. As indicated in Table 1, composites produced by this method had much improved
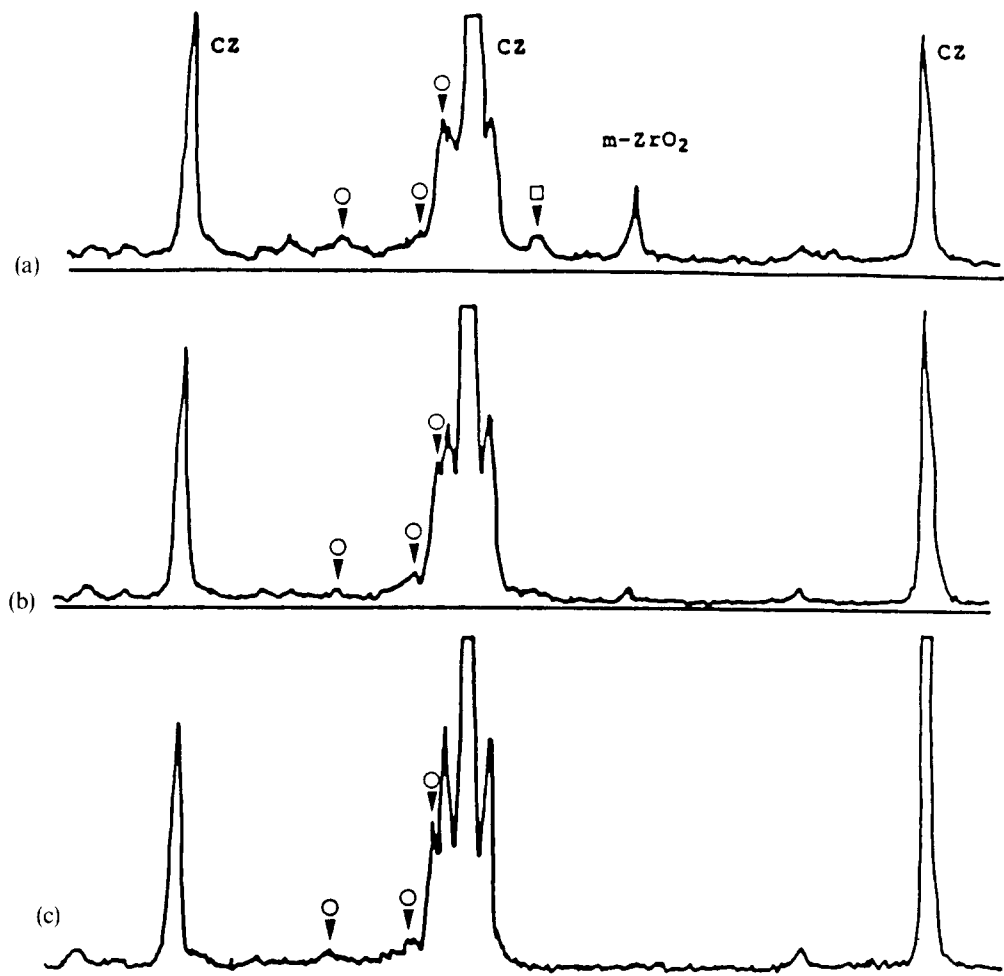

Fig. 3. XRD patterns following the phase evolution during reaction sintering of zircon and calcia. $\bigcirc$, β-Ca_2SiO_4; $\square$, $CaCO_3$. (a) 1000°C, 2 h; (b) 1100°C, 2 h; (c) 1200°C, 2 h.

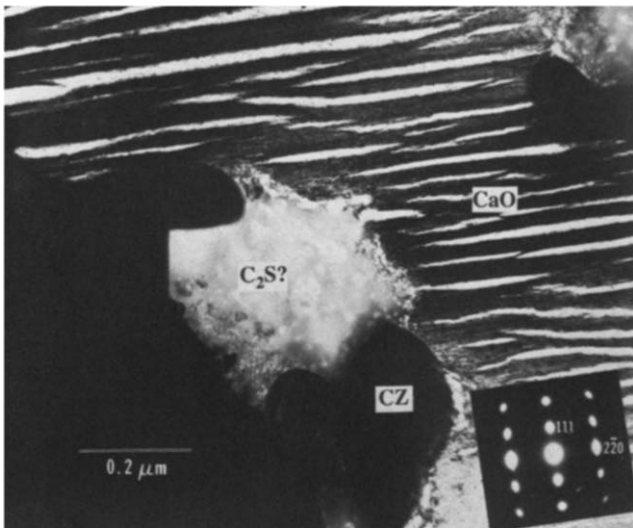**Fig. 4.** Bright field TEM micrograph of C₂S–CZ produced by the basic single-stage firing process.

density (4·03 g/cm³) and strength (~264 MPa) compared to those produced by the basic single firing process.

The basic microstructure of these composites is shown in Fig. 5 with a typical SEM backscatter image. Energy dispersive X-ray spectroscopy confirmed that the light contrast phase observed in Fig. 5 was CZ, but the dark contrast phase consisted of both C₂S and calcium-rich regions. Although the presence of these calcium-rich regions indicates that the C₂S-forming reaction was not completed in this process, no bulk regions of amorphous material were observed by TEM. Figure 6 is a transmission electron micrograph showing a grain of unreacted calcia adjacent to a grain of fully reacted C₂S with no bulk amorphous reaction layer between.

3.3 Alumina ball milled

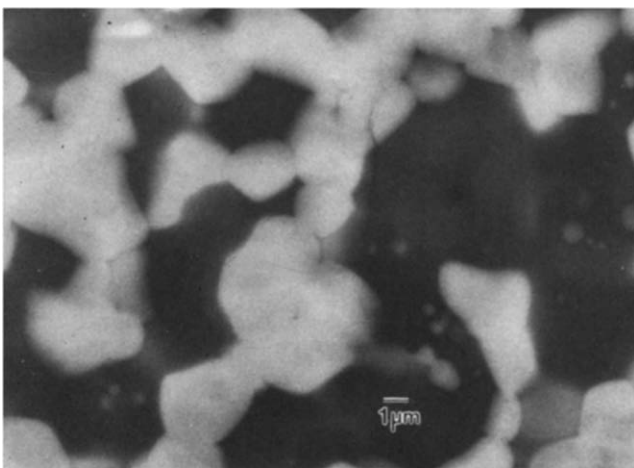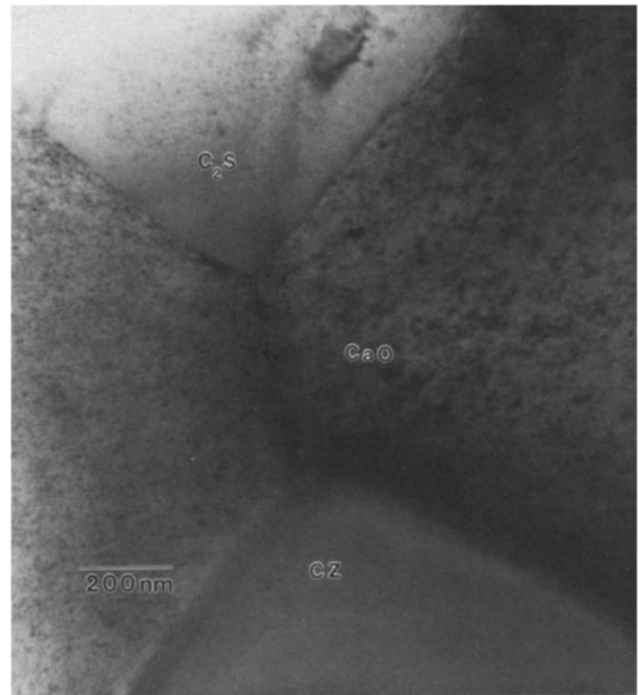As indicated in Table 2 approximately 0·15 wt% Al₂O₃ was incorporated into the starting powder

Fig. 6. Bright field TEM micrograph of unreacted calcia in a C₂S–CZ composite produced by the two-stage firing process.

because of the alumina milling media. The density (4·1 g/cm³) and strength (241 MPa) of these composites were comparable to those produced by the two-stage process (see Table 1). XRD results showed the presence of both majority CZ and minority C₂S phases. The basic microstructure of this composite is shown in Fig. 7, again with a scanning electron micrograph typical of the material..

Small regions of an amorphous phase were found in isolated pockets at multiple grain junctions. Where present, this phase appeared to be limited to the multiple grain junctions (as shown in Fig. 8(a) and (b)) and contained both calcium and significant
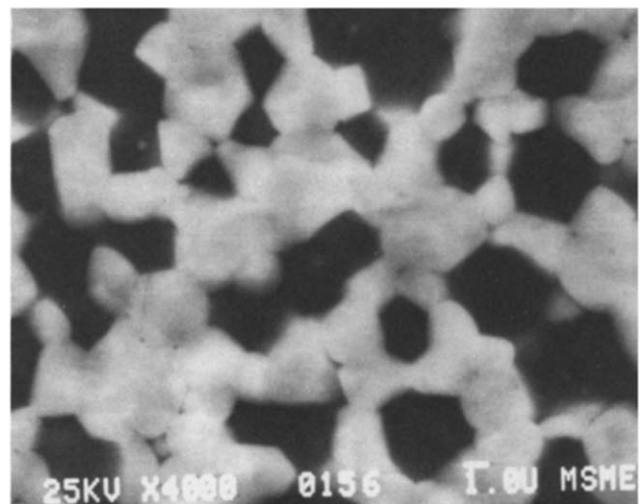

Fig. 5. Backscatter SEM micrograph of the C₂S–CZ composite produced by the two-stage firing process.

Fig. 7. Backscatter SEM micrograph of the C₂S–CZ composite produced by the single-stage firing process with alumina addition.
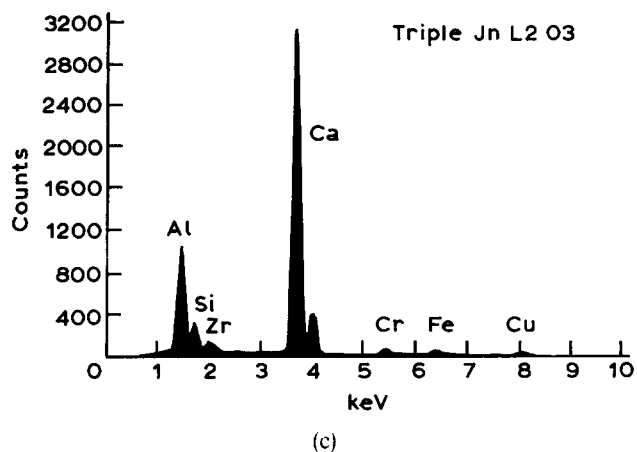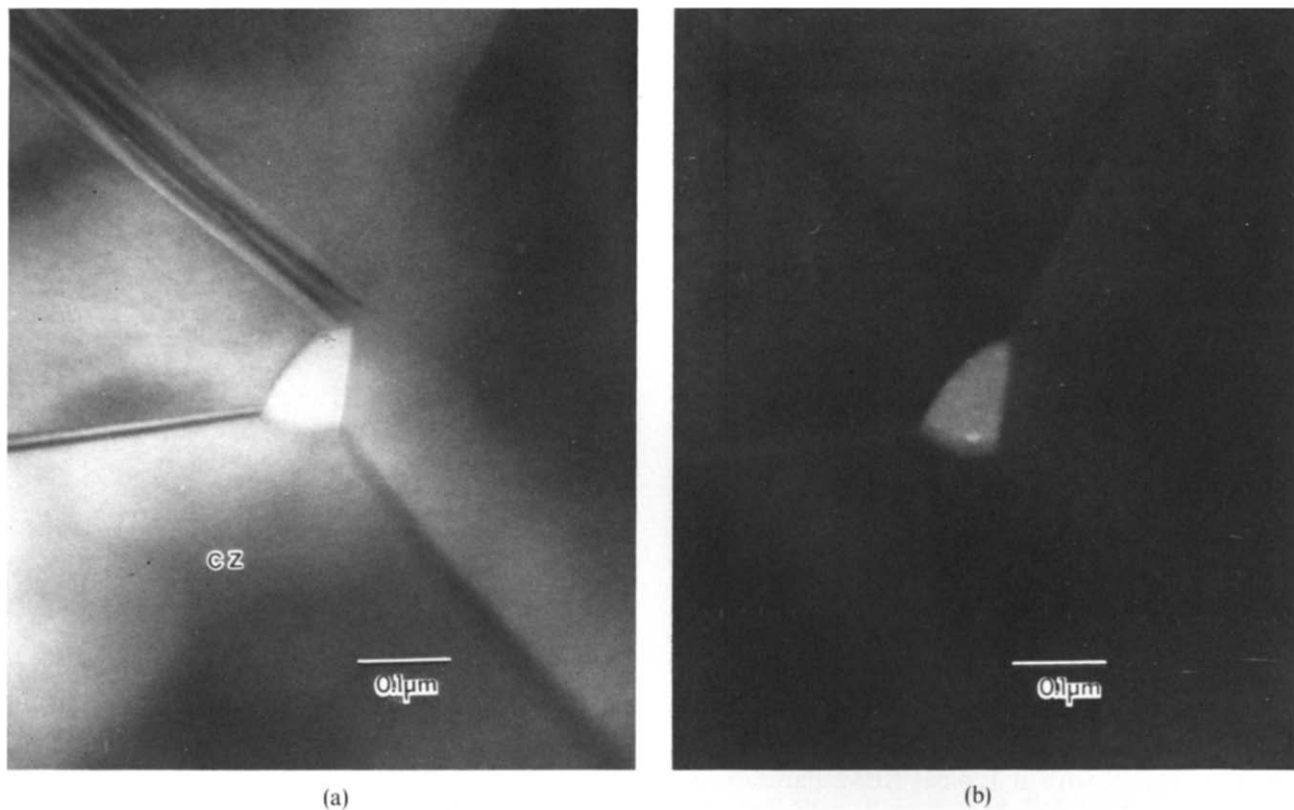
(a)

(b)

(c)

Fig. 8. Amorphous phase observed in an alumina-containing C_2S–CZ composite: (a) bright field TEM image; (b) dark field image of diffuse region of diffraction pattern; (c) typical EDS spectrum.

amounts of aluminum (as demonstrated in Fig. 8(c). No amorphous region could be located via TEM either by diffuse dark field imaging or by micro-diffraction along the extended grain boundaries. Aluminum was detected by EDS only in such amorphous phases.

4 Discussion

The three sintering processes result in composites with widely varying degrees of C_2S formation and yet all three have virtually complete CZ reaction. Additionally, the XRD results (Fig. 3) indicate significant amounts of CZ with but small amounts of

the desired C_2S at temperatures as low as 1000 and as high as 1200°C. Since the formation of C_2S is thus the limiting process during reaction sintering, particular attention must be paid to microstructural observations involving unreacted calcia or silica and any unexpected products.

The basic reaction scheme is unsuccessful due to the evolution of amorphous (non-stoichiometric) calcium silicate regions which inhibits the formation of C_2S, prevents further densification, and significantly degrades mechanical properties. Various calcium silicate reaction layers may be expected in the reaction of calcia and crystalline silica to form C_2S, but the amorphous nature of the silicate

reaction phases found in this experiment indicate the presence of significant kinetic barriers to the crystallization of C_2S. It is likely that the amorphous silicate products are the result in part of the amorphous nature of the silica source from plasma-decomposed zircon. The substitution of a crystalline silica source should not be expected to result in complete reaction with one firing, however, but rather in crystalline reaction layers as previously mentioned.

The two-stage firing scheme is much more successful as the rehomogenization step after the initial firing redistributed excess calcia and silica after CZ formation and the initial reactions forming amorphous silicates. This process did not result in a completely reacted composite because the rehomogenization, although removing the amorphous regions as reaction barriers about unreacted grains, does not address the broader problem of mass transport between regions of locally high calcia or silica content separated by the majority CZ phase.

The addition of alumina dopant (~ 0.15 wt%) through the attrition milling step significantly improved the single firing process, with strengths attained nearly as high as with the two-stage firing process. The improved strength attained relative to the basic reaction sintering process is attributed to the completion of the C_2S forming reactions with a corresponding decrease in the amount of low density amorphous phases. The factors which lead to the more complete reaction may be explained by examination of the relevant phase diagrams.

The sintering temperature in this process was sufficiently high that aluminum-rich melts may coexist with crystalline calcia, silica, CZ and calcium silicates.[7] As C_2S is the thermodynamically stable crystalline phase for the given stoichiometry, it crystallizes out of the melt as calcia and silica are dissolved. The formation of C_2S will continue until all available sources of unreacted calcia and silica are depleted, leaving behind small pockets of liquid residue. These pockets of liquid are quenched into the observed amorphous regions upon cooling due to the relatively low eutectic temperatures found in these systems. Such liquid phases are also likely to enhance the formation of CZ at these temperatures so that such amorphous regions are not restricted to either multiple C_2S or multiple CZ grain junctions.

Matrix constraint resulting from significant amounts of such alumina-rich glass has been used to explain the apparent stabilization of β-C_2S by alumina.[8] Although C_2S formation is essentially complete in this process, the impurity related amorphous regions may be responsible for the

apparent decrease in strength compared to composites produced by the two-stage firing process.

The successful use of a liquid-phase sintering agent to produce fully reacted composites should not be limited to the C_2S–CZ reaction sintering system. Similar low-temperature eutectics may be found in the Al_2O_3-poor regions of the CaO–SiO_2–MgO–Al_2O_3 system and might be used to advantage in the conventional or reaction sintering of C_2S–MgO composites.

5 Conclusions

The reaction sintering of calcia and plasma-decomposed zircon to form C_2S–CZ composite ceramics is limited by the formation of amorphous calcia- and silica-rich regions which inhibit the formation of C_2S. This problem may be partially remedied by prereaction and rehomogenization of the starting powders or by adding small amounts of alumina ($< 1\%$) which is believed to form a liquid phase with high calcia and silica solubilities during sintering.

Composites produced by a two-stage reaction sintering process are found to have the highest bend strengths (~ 264 MPa), but the presence of calcia grains indicates that these composites were not fully reacted. Similar strengths (~ 241 MPa) were obtained by the addition of alumina during attrition milling and such composites showed complete C_2S formation with no excess calcia. The addition of alumina as a sintering additive may be useful as a liquid-phase sintering agent but deleterious as an amorphous phase former.

References

1. Moya, J. S., Pena, P. & De Aza, S., Transformation toughening in composites containing dicalcium silicate. *J. Am. Ceram. Soc.*, **68** (1985) C259–C262.
2. Quereschi, M. H. & Brett, N. H., Phase equilibria in ternary systems containing zirconia and silica. I. The system CaO–ZrO_2–SiO_2. *Trans. Brit. Ceram. Soc.*, **67** (1968) 205–19.
3. Sircar, A., Brett, N. H. & White, J., Phase studies in the system CaO–MgO–ZrO_2–SiO_2. *Trans. Brit. Ceram. Soc.*, **77** (1978) 77–8.

4. Taylor, D., Thermal expansion data. VII. Complex oxides AB$_2$O$_4$. *Brit. Ceram. Trans. J.*, **83** (1984) 149.
5. Evans, A. M. & Williamson, J. P. H., Composition and microstructure of dissociated zircon produced in a plasma furnace. *J. Mat. Sci.*, **12** (1977) 779–90.
6. Wong, A. M. & McPherson, R., The structure of plasma decomposed zircon, *J. Mat. Sci.*, **16** (1981) 1732–5.
7. Pena, P. & De Aza, S., Compatibility relations of Al$_2$O$_3$ in the system ZrO$_2$–Al$_2$O$_3$–SiO$_2$–CaO. *J. Am. Ceram. Soc.*, **67** (1984) C3–5.
8. Chan, C., Kriven, W. M. & Young, J. F., Analytical electron microscopic studies of doped dicalcium silicates. *J. Am. Ceram. Soc.*, **71** (1988) 713–19.